Rate coefficients and kinetic isotope effects of the Cl + XCl → XCl + Cl (X=H, D, Mu) reactions from ring polymer molecular dynamics→

Junhua Fang,[a] Wenbin Fan,[b] Hui Yang,[b] Jianing Song[b*] and Yongle Li[b,*]

[a] *Department of Chemistry, Shanghai University, Shanghai 200444, China*

[b] *Department of Physics, International Center for Quantum and Molecular Structures, and Shanghai Key Laboratory of High Temperature Superconductors, Shanghai University, Shanghai 200444, China*

The ring-polymer molecular dynamics (RPMD) was used to calculate the thermal rate coefficients and kinetic isotope effects of the heavy-light-heavy abstract reaction Cl + XCl → XCl + Cl (X=H, D, Mu). For the Cl + HCl reaction, the excellent agreement between the RPMD and experimental values provides a strong proof for the accuracy of the RPMD theory. And the RPMD results also consistent with results from other theoretical methods including improved-canonical-variational-theory and quantum dynamics. The most novel finding is there is a double peak in Cl + MuCl reaction near the transition state, leaving a free energy well. It comes from the mode softening of the reaction system at the peak of the potential energy surface. Such an explicit free energy well suggests strongly there is an observable resonance. And for the Cl + DCl reaction, the RPMD rate coefficient again gives very accurate results comparing with experimental values. The only exception is at the temperature of 312.5 K, at this temperature, results from RPMD and all other theoretical methods are close to each other but slightly lower than the experimental value, which indicates experimental or potential energy surface deficiency.

Key words: Ring-polymer MD, Quantum effects, Recrossing effects, Reaction rate coefficient, Kinetic isotope effect

*Corresponding authors.

E-mail address: js888@shu.edu.cn (JS) and yongleli@shu.edu.cn (YL).

I. INTRODUCTION

In the study of chemical kinetics, the rate coefficient of chemical reactions is an essential observable. It plays a key role in the investigations of combustion, atmospheric and interstellar chemistry. Because experimental measurement of rate coefficients is usually expensive and inaccurate under certain conditions, theoretical calculation is indispensable. The theoretical calculations not only provide comparison with experimental data, but also provide a basis for understanding reaction mechanisms and assess the underlying potential energy surface (PES).

Classical molecular dynamics provides direct observation of reaction process, giving intuitions of the reaction mechanism. But due to lack of quantum effects, such as zero-point energy (ZPE) and quantum tunneling, it is only reliable for estimation the rate coefficients of reactions containing only heavy atoms and at high temperatures. On the other hand, although the methods based on quantum mechanics, such as quantum scattering with wave packet, can give much accurate rate coefficients, for systems containing multiple atoms, say, more than seven, accurately solving the quantum scattering Schrödinger equation is a mission impossible [1-4]. Thus, in the past few decades, many approximate quantum mechanical simulation techniques have been proposed to calculate the reaction rate coefficients, and some methods can be used for

full-dimensional calculations of more complex systems [5-9].

The transition state theory (TST) proposed around 1930s was the first attempt for a balance between accuracy and efficiency [10, 11]. At the same time, some of its approximate semi-empirical revisions can also capture the quantum effects in the reaction, such as quantum transient theory [8, 12], but those methods still have many non-negligible shortcomings. The TST method assumes that there is a dividing surface separating the reactants and products, so it ignores the recrossing in dynamical effects, and it is also difficult to find an accurate dividing surface, especially for high-dimensional or barrier-less reactions. Another difficulty is it can hardly handle the multi-dimensional tunneling effect within the TST framework. Also, at high temperatures, the recrossing of some complex reactions are essentially unavoidable, especially in heavy-light-heavy mass combination reactions.

Another compromise is the quasi-classical trajectory (QCT) method. QCT uses quantum mechanics for assigning initial energy, but classical mechanics for propagating the trajectories. So although the recrossing in dynamical effects is naturally included in the QCT trajectories, quantum effects such as tunneling have been totally ignored, so the results are unreliable in cases which quantum effects playing significant roles, especially under low energy and temperature conditions [13, 14]. Another problem for QCT is the ZPE leakage [15, 16].

Recently, there is a reliable and effective alternative to the above methods, the ring-polymer molecular dynamics (RPMD), developed by the Manolopoulos group [17, 18]. RPMD is a full-dimensional approximation dynamic method that covers many quantum features ignored in other methods, and is adopted to study the chemical reaction rate coefficients in this work. It uses the imaginary time path integral formalism, and utilizes isomorphism between the quantum statistical mechanics of a physical systems and the classical statistical mechanics of a fictitious system in which each particle is depicted as a ring of beads connected by harmonic interaction [17]. In recent years, this method has been effectively applied to calculate the rate coefficient of gas phase bi-molecular reactions, and can give accurate results and shows advantages as follow: At the high temperature limit, the RPMD values become accurate [18], and the ring-polymer disintegrates into individual beads. It can conserve the ZPE along the reaction path in the calculation [19], and correctly simulate the ZPE. And the method has a well-defined short-time limit, which gives a theoretical upper limit of the quantum TST rate for the RPMD rate [20]. It also provides a precise solution for parabolic barriers. At last, since RPMD rate coefficients are based on the long-term limit of the correlation function, it does not depend on the choice of position of the dividing surface [9], which is a great advantage for the low-barrier and barrier-less systems without a clear interface.

In this work, we calculate the thermal rate coefficients and kinetic isotope effects (KIEs) for the Cl + XCl $\rightarrow$ XCl + Cl (X=H, D, Mu) reaction, using RPMD. Here, Mu has a mass of 0.113 u and lifetime of 4 μs. It is the shortest lived and the lightest hydrogen isotope composed of positive ions and electrons ($Mu=\mu^{+}e^{-}$). It is the most sensitive probe for quantum mass effects in chemical reactions [21, 22]. This system is a typical heavy-light-heavy mass combination with the transfer of hydrogen atom. In particular, this mass combination gives the reaction a very small skewing angle characteristic, so there is a significant recrossing and tunneling in this system. Therefore, this reaction has certain research value in reaction dynamics. In this work, we investigate the rate of the hydrogen exchange channel, and then compare the RPMD rate coefficients and KIEs with other published results. The remainder of this article is arranged as follows: The second part briefly introduces the RPMD theory and computational details, the third section presents and discusses the calculation results, and the fourth section gives the conclusions.

II. METHOD

A RPMD theory

In this work, we use the package RPMDrate for obtaining the rate coefficients, which was released by Y.V.S et al [23].The entire theory and computational options are described in detail elsewhere, especially in [23]

and [24], so here we only give a brief summary. For a three-atom reaction, its quantum Hamiltonian can be expressed as follows:

$$\hat{H} = \sum_{i=1}^{3} \frac{|\hat{p}_i|^2}{2m_i} + V(\hat{q}_1, \hat{q}_2, \hat{q}_3) \quad (1)$$

Where $\hat{p}_i$ and $\hat{q}_i$ represent the momentum and Cartesian coordinate operators of the i_{th} atom respectively; and the m_i represents the mass of that atom. In the RPMD rate theory, single atom is replaced by a ring-polymer with n classical beads, so the corresponding isomorphic n-beads classical Hamiltonian is:

$$H_n(\vec{p}, \vec{q}) = \sum_{i=1}^{3} \sum_{j=1}^{n} \left(\frac{\left|\vec{p}_i^{\,(j)}\right|^2}{2m_i} + \frac{m_i \omega_n^2}{2} \left|\left| \vec{q}_i^{\,(j)} - \vec{q}_i^{\,(j-1)} \right|\right|^2 \right) + \sum_{j=1}^{n} V\left(\vec{q}_1^{\,(j)}, \vec{q}_2^{\,(j)}, \vec{q}_3^{\,(j)}\right) \quad (2)$$

In the above formula $\vec{q}_i^{(0)} = \vec{q}_i^{(n)}$, and $\omega_n = (\beta_n \hbar)^{-1}$ is the force constant between two neighboring beads, $\beta_n = \beta/n = (nk_BT)^{-1}$ is related to the temperature of the system, and k_B is the Boltzmann constant. Two dividing surfaces are used for determining the reaction coordinate. The first one is located in the reactant asymptote valley [24]:

$$s_0\left(\overline{\vec{q}}\right) = R_\infty - \left|\overline{R}\right| \quad (3)$$

In the above formula, $\left|\overline{R}\right|$ is the centroid distance between the centers of the mass (COM) of the two reactants, another parameter R_∞ is a pre-defined distance between the two reactions, which is generally large enough to ensure that there is no interaction between them. Another dividing surface is set at the vicinity of the transition state (TS), and the title system have two equivalent product arrangement channels [23]:

$$s_1\left(\overline{\vec{q}}\right) = \max\left\{s_{\mathrm{B}}\left(\overline{\vec{q}}\right), s_{\mathrm{C}}\left(\overline{\vec{q}}\right)\right\} \tag{4}$$

Where

$$s_{\mathrm{B}}\left(\overline{\vec{q}}\right) = \left(\left|\overline{\vec{q}}_{\mathrm{BC}}\right| - q_{\mathrm{BC}}^{\neq}\right) - \left(\left|\overline{\vec{q}}_{\mathrm{AB}}\right| - q_{\mathrm{AB}}^{\neq}\right) \tag{5}$$

and

$$s_{\mathrm{C}}\left(\overline{\vec{q}}\right) = \left(\left|\overline{\vec{q}}_{\mathrm{BC}}\right| - q_{\mathrm{BC}}^{\neq}\right) - \left(\left|\overline{\vec{q}}_{\mathrm{AC}}\right| - q_{\mathrm{AC}}^{\neq}\right) \tag{6}$$

Here $\overline{\vec{q}}_{\mathrm{BC}}$ is the vector connects the centroids of atom B and C, Another parameter $q_{BC}^{\neq}$ is the distance between B and C at the TS. The meaning of $\overline{\vec{q}}_{\mathrm{AC}}$ and $q_{\mathrm{AC}}^{\neq}$ is similar. The final reaction coordinate ξ can be expressed as functions related to $s_0\left(\overline{\vec{q}}\right)$ and $s_1\left(\overline{\vec{q}}\right)$:

$$\xi\left(\overline{\vec{q}}\right) = \frac{s_0\left(\overline{\vec{q}}\right)}{s_0\left(\overline{\vec{q}}\right) - s_1\left(\overline{\vec{q}}\right)} \tag{7}$$

So it's clear that $\xi \to 0$ as $s_0 \to 0$ and $\xi \to 1$ as $s_1 \to 0$.

Finally, the formula of RPMD rate coefficient is given in the form of Bennett-Chandler factorization [25, 26]:

$$k_{\mathrm{RPMD}} = k_{\mathrm{QTST}}(T; \xi^{\neq})\kappa(t \to \infty; \xi^{\neq}) \tag{8}$$

Here the two terms represent the static contribution and dynamical correction respectively. The first one $k_{\mathrm{QTST}}(T; \xi^{\neq})$ is the centroid-density quantum transition-state theory (QTST) rate coefficient, calculated from the top position of the free energy barrier along the reaction coordinate $\xi(q)$. In practice, The first factor is calculated from the potential of mean force (PMF) along ξ [24, 27]:

$$k_{\mathrm{QTST}}(T;\xi^{\neq}) = 4\pi R_{\infty}^{2}\left(\frac{m_{\mathrm{A}}+m_{\mathrm{B}}}{2\pi\beta m_{\mathrm{A}}m_{B}}\right)^{1/2} e^{-\beta[W(\xi^{\neq})-W(0)]} \quad (9)$$

In the above formula, $W(\xi^{\neq}) - W(0)$ is the free-energy difference can be calculated by umbrella integration [28].

The second factor $\kappa(t \to \infty;\xi^{\neq})$ is dynamical correction, which accounts for recrossing of the transition-state dividing surface. It is represented by the ratio of two flux-side correlation functions:

$$\kappa(t \to \infty;\xi^{\neq}) = \frac{c_{fs}^{(n)}(t\to\infty;\xi^{\neq})}{c_{fs}^{(n)}(t\to 0_{+};\xi^{\neq})} \quad (10)$$

So it is the ratio of the long-term limit and the zero-time limit of the flux-side correlation function, and provides dynamic correction of k_{QTST}, which captures the recrossing of the TS region and ensures that the obtained RPMD rate coefficient result k_{RPMD}(T) is not dependent on the choice of the dividing surface [23, 24, 29].

It should be noted that the final RPMD rate coefficient of the chemical reaction in this article also needs to be multiplied by the electronic degeneracy factor $f(T)$, in order to take into account the spin-orbit splitting of Cl($^{2}\mathrm{P}_{1/2,3/2}$), with the splitting energy $\Delta\mathrm{E} = 882$ cm^{-1}. As mentioned in previous work on Cl + HCl [29], the final RPMD rate coefficients were corrected with an electronic partition function ratio of the following form:

$$f(T) = \frac{Q_{\mathrm{elec}}^{\mathrm{TS}}}{Q_{\mathrm{elec}}^{\mathrm{reactants}}} = \frac{1}{2+\exp(-\beta\Delta E)} \quad (11)$$

In the calculation of the RPMD rate theory, when only one bead is used, it falls to the classical limit [27]. It is therefore possible to evaluate

the limits of quantum effects such as ZPE and tunneling in the simulation by using enough beads, and the more beads used, the more accurate the calculated rate constant values. And each simulation system has the minimum number of beads [30]:

$$n_{\min} = \beta\hbar\omega_{\max} \tag{12}$$

Where $\omega_{\max}$ is the maximum vibrational frequency in the reaction system. In this work, it is the frequency of H-Cl stretching. There is also a key variable, the crossover temperature: $T_c = {\hbar\omega_b}/{2\pi k_B}$, where $i\omega_b$ is the imaginary frequency of the TS. The temperature lower than T_c is generally regarded as the deep-tunneling region [31], and RPMD results becomes with larger error in this temperature region. In that work [31],the authors summarized through some benchmark model systems, finding the estimation of deviation of RPMD results at deep tunneling region. That is, due to the interaction between the excited bead-bead vibrational modes and physical centroid modes below T_c , when the potential energy barrier on PES is symmetric RPMD would underestimate the rate coefficients, while if the barrier is asymmetric, RPMD would overestimate it. And such deviation of RPMD below T_c was later validated in the reaction Mu + H_2 [32] and H/D/Mu + CH_4 [33].

B Computational details

We collect all the detailed calculation parameters used in this work in Table I. In all the calculations we used the Bondi–Connor–Manz–

Römelt (BCMR) PES for Cl + HCl reaction [34]. The masses of the relevant atoms in the reaction were selected as follows: m_{H} = 1.007825, m_{D} = 2.014101, m_{Mu} = 0.113 and m_{Cl} = 34.96885, using the atomic mass units. The skewing angle is calculated as [35] :

$$\phi = \arctan\sqrt{\frac{m_{\mathrm{B}}M}{m_{\mathrm{A}}m_{\mathrm{C}}}} \tag{13}$$

Where $M = m_{\mathrm{A}} + m_{\mathrm{B}} + m_{\mathrm{C}}, m_{\mathrm{B}}$ is the mass of X atom. So after inserting the corresponding atomic masses, the skewing angles of reaction Cl + HCl, Cl + DCl, and Cl + MuCl are 13.6°, 18.9°, and 4.7° separately. Here it can be seen the skew angles for all the three reactions are very small, especially for the Cl + MuCl system. So there would be significant recrossing at the TS region.

The temperatures used are in the range of 200 K~1500 K, 128 beads were used at T < 600 K, and 32 beads were used at T ≥ 600 K. As mentioned above, we calculated the rate coefficients for each reaction with one bead at different temperatures, to obtain the classical limit, and then calculated them with multiple beads. When calculating the PMF profiles, the reaction coordinates are divided into a series of windows. For all the reactions, the range of reaction coordinate is set as $\xi \in [-0.05, 1.10]$, so the total number of windows is 115. To ensure the overlap of distributions of reaction coordinates between windows, the intervals between neighboring windows is set as 0.01. For the three reactions, the force constants are all set to k = 2.727 (T/K) eV. In all

simulations, Andersen thermostat [36] was used.

After the PMF in each system was obtained, the transmission coefficient is calculated. First, the SHAKE algorithm [37] was used to fix the ring-polymer centroid at the free energy barrier, and a long parent trajectory is run. The configuration was sampled every 3 ps to be used as the initial position of the child trajectories for obtaining the flux-side correlation function. For each initial position, 100 individual ring-polymer trajectories with different initial momentum are sampled from reach the Boltzmann distribution, and these trajectories will propagate 3 ps without restriction, which is enough for the transmission coefficients reach to their equilibrium. For all the calculations, the time interval is set to 0.1 fs.

III. RESULTS AND DISCUSSION

In RPMD calculations, the number of beads needed depends on different temperatures and isotopes, and the number of beads is not less than the minimal value suggested by Eq. (11). The rate coefficients calculated by RPMD method, other theoretical methods, and measured from experiments are collected in Table II.

And the minimum energy path (MEP) is shown in FIG. 1. The notion a, b, and c represent the MEP of reactions Cl + HCl, Cl + DCl, and Cl + MuCl, respectively. For the MEP, all the three reactions are similar, and all are symmetric due to the same heavy atoms used. But for the Cl +

MuCl, the barrier is rather sharp due to the definition of the rection coordinate s is mass-scaled [38]. For the ground state adiabatic energy ($V_a^G(s)$), which defined as potential energy plus ZPE, it can be seen explicitly the significant double well feature from all of the three reactions. This is from the combination of softening of the X-Cl (X=H, D, Mu) stretching and hardening of the two modes perpendicular to line connecting the two Cl atoms along the MEP from reactant to the TS (Shown in the supplementary information FIG. S1).

The three curves are also different greatly due to the difference in ZPE, especially the Cl + MuCl reaction. In that system, the double adiabatic ground-state energy well at the TS region are as deep as about 7 kcal·mol^{-1}, separated by a very low barrier (1 kcal·mol^{-1}). This feature is highly similar as observed in the reaction system Cl + HD [39], but in that case, the driving force of formation of the energy well at TS region is the softening of vibrational excited state ($n=1$) of the Cl-H stretching mode, other than the softening of the ground state of Cl-Mu stretching mode here. And this significant mode softening in Cl + MuCl reaction system suggests there also would be strongly reactive resonance in it. We hope further investigations can prove this.

The figures in the left panel of FIG. 2 shows the PMF of the Cl + XCl (X=H, D, Mu) reactions at temperature 312.5 K. The converged RPMD barriers of all three reactions are lower than the classical results.

This is apparent since the tunneling effect makes all three isotopes easier penetrate the potential energy barrier. And the sequence of free energy lowered of the barriers is: $\Delta G_{\mathrm{D}} < \Delta G_{\mathrm{H}} < \Delta G_{\mathrm{Mu}}$ according to the decreasing of the mass of these isotopes. This sequence comes from the less of mass, the larger of the tunneling ability. For the case of isotope Mu, the PMF curve is more interesting that the RPMD PMF barrier splits into double peaks, separated by a free energy well. As the temperature increases, the potential energy double peak of the reaction maintains to as high as 1000 K, and then smear out at 1500 K, leaving a wide flat peak, as shown in the supplementary information FIG. S2. But the highest free energy peak of the Cl + MuCl reaction approaches gradually to the TS, from $\xi = 1.07$ to $\xi = 1.0$. This is an explicit evidence of quantum effect, since in quantum mechanics, the ground state of a double well is the system reside at the middle of the central energy barrier, with each well a half, and with the energy lower than that barrier [40, 41]. But from the classical mechanics, the system cannot stay at the middle of the double well. In previous RPMD calculations, it's well known the quantum tunneling can cause the free energy barrier shifting, lowering and broadening [32, 42, 43], but the single peak split into double ones is seldom.

The right panel of FIG. 2 shows corresponding transmission coefficients at the same temperature over time. The transmission

coefficients of these three reactions converge fast with time (20~30 fs). The transmission coefficient $\kappa(t \to \infty)$ (denoted as κ below) for Cl + HCl and Cl + DCl is 0.42 and 0.63, respectively. Since the mass is larger for D, it exhibits less tunneling and recrossing, leading to a larger κ. For the Cl + MuCl, κ is the smallest, reduced to 0.12. That again means Mu with a significant recrossing at the TS region. From the plots, there are also some oscillations in both the classical and RPMD transmission coefficients of the Cl + MuCl reaction. This is due to the coupling between some vibrational mode to the reaction coordinate at given dividing surface, which is similar to the previous Mu + H_2 [32, 42, 43] and H + CH_4 [33] reaction, and without physical meaning. Table 2 that the converged RPMD transmission coefficients increase with increasing temperature, which indicates that there are more recrossing at low temperatures, this is consistent with previous studies [24, 29].

FIG. 3 illustrates the Arrhenius plot of the RPMD rate coefficients of the Cl + HCl reaction compared with experimental values and other theoretical results. The results from improved canonical variational theory (ICVT) rate constants with quantum correction of Garrett et al [44] (ICVT/LCG), showed a large deviation between two sets of previous results, denoted as ICVT/LCG^1 and ICVT/LCG^2, this would stem from the different PESs and VTST parameters are used. The QD results from exact quantum reaction scattering done by Collepardo-Guevara et al. [45].

The experimental results are collected in the work of Garrett et al. [44] and is denoted as Expt. In the RPMD results, the RPMD/Conv represents the rate coefficient calculated under the converged number of beads. RPMD/1bead represents RPMD results from single bead. As shown in the Fig.3, the converged RPMD rate coefficients agree well with both the experimental and QD results at temperatures above 312.5 K, while below 312.5 K, RPMD results are slightly lower than those from QD and ICVT/LCG^2. But all theoretical results are slightly larger than the experimental value at 423.2 K (about 13%). This singular value would result from either the experimental error, or deficiency of the PES we used, since the crossover temperature T_C [46] for Cl + HCl is about 320 K, and RPMD results are reliable at the temperatures above T_C.

The rate coefficients of the Cl + DCl reaction at different temperatures are depicted in FIG. 4. Again there is a large deviation between the two sets of ICVT results, and the convergent RPMD rate coefficients are very close to those from ICVT/LCG^2. Here one can also observe that RPMD rate coefficients are in good agreement with the experimental values, with only exception at 312.5 K (deviation is about 33%). It can be inferred again the deviation stems from the experimental error or PES, since the T_C of Cl + DCl is about 228 K, the 312.5 K is again in accurate region for RPMD results.

For the Cl + MuCl reaction, since there is no relevant experimental

values, its RPMD calculation results are listed in Table II only. But under the given PES, the deviation from future experimental work would be larger, since the T_C for Cl + MuCl is as high as 950 K, the results under that temperature are all in deep tunneling region. This can also explain the double well feature of PMF of Cl + MuCl at 312.5 K, in such a deep tunneling region caused the reaction system of Cl + MuCl exhibits more quantum ground state feature than the H and D cases [47-49].

The KIE of the H and D isotopes are shown in FIG. 5, where the experimental values are copied from those collected by Garrett et al [44], Other theoretical values can be found in Bondi's work [50], including TST, ICVT and quantum dynamics (QD) results. It can be seen from the figure that the KIE values (1~20) weaken much with the temperature increasing, and converge to 1 when temperature higher than 1000 K. Except obtained from TST, the theoretical values are close to each other, and slightly lower than the experimental values by about 10%. The exceptional values at 312.5 K appear again, and are systematically lower than the experimental one as about 37%. As discussed above, this outlier may be from either the deficiency of PES used in this work, or the experimental error, and cannot be canceled out when calculating KIE. We hope future PES of Cl + HCl with higher accuracy can settle down this problem.

IV. CONCLUSION

In this work, we used the full-dimensional approximate quantum mechanics method RPMD to calculate the rate coefficients and KIEs of the typical symmetric heavy-light- heavy abstract reactions Cl + XCl $\rightarrow$ XCl + Cl (X=H, D, Mu) in the temperature range 200 K~1500 K. It is shown that these reactions are strongly influenced by recrossing and quantum mechanical effects. Especially, we found the reaction system of Cl + MuCl exhibit quantum ground state feature which split free energy barrier into a double peak with a well at the TS region along the reaction coordinates. From detailed analysis, we also found the peak splitting stems from the double well formation of the PMF along the reaction coordinate, caused by mode softening of the X-Cl stretching, and mode hardening of the two out-of-Cl-Cl-line modes (Shown in the supplementary information FIG. S1).

For both the Cl + HCl and Cl + DCl reactions, the RPMD rate coefficients are generally in good agreement with QD results and experimental results. But the deviations between theoretical results and experimental values for the two reactions at 312.5 K are exceptionally larger. This large deviation also causes the large deviation of RPMD KIE value to the experimental value. For Cl + MuCl, we provide a comparison for further experimental work, but since our results are in deep tunneling region of Cl + MuCl, they might be with larger deviation from

experimental values than in the H/D cases.

In short, the rate coefficients and KIEs results calculated by RPMD are not only in good agreement with the QD results, but also overall agreement with the experimental results. These results indicate that RPMD provides a reliable means of obtaining rate coefficients. And we also illustrate RPMD can reveal quantum ground state for the reaction system within a double well at TS region, caused by mode softening. But still we find there is a strange exception temperature, at which the deviation between RPMD results and experimental values deviate exceptionally large. Further work is needed such as constructing a new PES, to approve the evidence of accuracy from RPMD calculations.

V. ACKNOWLEDGEMENTS

This study was funded by the National Nature Science Foundation of China (No. 21503130 and 11674212 to Y.L., and 21603144 to J.S.). Y.L. is also supported by the Young Eastern Scholar Program of the Shanghai Municipal Education Commission (QD2016021) and the Shanghai Key Laboratory of High Temperature Superconductors (No. 14DZ2260700). J.S. is also supported by Shanghai Sailing Program (No. 2016YF1408400). Part of the calculations has been done on the supercomputing system, Ziqiang 4000, in the High Performance Computing center in Shanghai University. And Y.L. thanks Bin Jiang for his helpful discussions.

TABLE I. Input parameters for the RPMD calculations on title reactions.

Parameter	Reaction		Explanation
Cl + XCl (X=H, D, Mu)			
Command line parameters			
	200		
	300		
	312.5	600	
Temp	358	1000	Temperature(K)
	368.2	1500	
	400		
	423.2		
N_{beads}	128	32	Number of beads
Dividing surface parameters			
R_{∞}	15		Dividing surface s_1 parameter (a_0)
N_{bonds}	1		Number of forming and breaking bonds
N_{channel}	1		Number of equivalent product channels
Thermostat	'Andersen'		Thermostat option
Biased sampling parameters			
N_{windows}	115		Number of windows
ξ_1	-0.05		Center of the first window
$\mathrm{d}\xi$	0.01		Window spacing step
ξ_{N}	1.10		Center of the last window
$\mathrm{d}t$	0.0001		Time step (ps)
$N_{\mathrm{trajectory}}$	100		Number of trajectories
$t_{\mathrm{equilibration}}$	20		Equilibration period (ps)
t_{sampling}	100		Sampling period in each trajectory (ps)
Potential of mean force calculation			
ξ_0	−0.02		Start of umbrella integration
$\xi_{\ddagger}$	1.09		End of umbrella integration
N_{bins}	5000		Number of bins
Recrossing factor calculation			
$\mathrm{d}t$	0.0001		Time step (ps)
$t_{\mathrm{equilibration}}$	20		Equilibration period (ps) in the constrained (parent) Trajectory
$N_{\mathrm{totalchild}}$	1000000		Total number of unconstrained (child) trajectories
$t_{\mathrm{childsampling}}$	3		Sampling increment along the parent trajectory (ps)
N_{child}	100		Number of child trajectories per one initially constrained Configuration
t_{child}	3		Length of child trajectories (ps)

TABLE II. Compare the RPMD rate coefficients (unit: $cm^3\ s^{-1}$) of the Cl + XCl (X=H, D, Mu) reactions with other published experimental and theoretical results, and the unit for the PMF is eV in this table. Experimental values k_{expt} and theoretical calculation results k_{ICVT/LCG^2} from reference [44].

T/K	200	300	312.5	358	368.2	400	423.2	600	1000	1500
Cl + HCl										
N_{beads}	128	128	128	128	128	128	128	32	32	32
$\xi^{\neq}$	0.999	1.000	1.000	1.000	1.000	0.999	1.000	0.999	1.000	1.000
$\Delta G(\xi^{\neq})$	0.333	0.396	0.402	0.432	0.434	0.452	0.466	0.555	0.732	0.917
k_{QTST}	1.45× 10^{-17}	9.82× 10^{-16}	1.48× 10^{-15}	4.04× 10^{-15}	5.77× 10^{-15}	1.06× 10^{-14}	1.49× 10^{-14}	1.36× 10^{-13}	1.66× 10^{-12}	8.19× 10^{-12}
κ	0.368	0.410	0.417	0.440	0.442	0.454	0.463	0.505	0.546	0.542
k_{RPMD}	2.67× 10^{-18}	2.00× 10^{-16}	3.05× 10^{-16}	8.774 ×10^{-16}	1.26× 10^{-15}	2.35× 10^{-15}	3.37× 10^{-15}	3.25× 10^{-14}	3.97× 10^{-13}	1.83× 10^{-12}
k_{expt}	---	---	(1.5± 0.8)× 10^{-15}	(4.2± 2.5)× 10^{-15}	(5.1± 2.4)× 10^{-15}	---	(1.5± 0.6)× 10^{-14}	---	---	---
k_{ICVT/LCG^2}	1.70× 10^{-17}	7.50× 10^{-16}	1.00× 10^{-15}	2.70× 10^{-15}	3.30× 10^{-15}	5.60× 10^{-15}	7.80× 10^{-15}	4.70× 10^{-14}	3.00× 10^{-13}	9.00× 10^{-13}
Cl + DCl										
N_{beads}	128	128	128	---	128	128	128	32	32	32
$\xi^{\neq}$	0.999	1.000	0.999	---	0.999	0.999	1.000	0.999	1.000	0.999
$\Delta G(\xi^{\neq})$	0.378	0.439	0.447	---	0.477	0.493	0.506	0.588	0.751	0.926
k_{QTST}	6.74× 10^{-19}	1.19× 10^{-16}	1.78× 10^{-16}	---	9.15× 10^{-16}	2.00× 10^{-15}	3.15× 10^{-15}	4.58× 10^{-14}	8.35× 10^{-13}	4.88× 10^{-12}
κ	0.585	0.637	0.634	---	0.640	0.646	0.649	0.655	0.646	0.634
k_{RPMD}	1.97× 10^{-19}	3.76× 10^{-17}	5.60× 10^{-17}	---	2.88× 10^{-16}	6.32× 10^{-16}	1.00× 10^{-15}	1.42× 10^{-14}	2.37× 10^{-13}	1.28× 10^{-12}
k_{expt}	---	---	(1.7± 0.9)× 10^{-16}	---	(1.0± 0.5)× 10^{-15}	---	(3.6± 1.6)× 10^{-15}	---	---	---
k_{ICVT/LCG^2}	1.60× 10^{-18}	1.60× 10^{-16}	2.40× 10^{-16}	7.80× 10-16	9.80× 10^{-16}	1.90× 10^{-15}	2.80× 10^{-15}	2.30× 10^{-14}	2.10× 10^{-13}	7.30× 10^{-13}
Cl + MuCl										
N_{beads}	128	128	128	---	---	128	---	32	32	32
$\xi^{\neq}$	1.070	1.068	1.067-	---	---	1.061	---	1.047	0.978	1.002
$\Delta G(\xi^{\neq})$	0.155	0.191	0.196	---	---	0.227	---	0.301	0.442	0.627

k_{QTST}	7.25× 10^{-13}	4.66× 10^{-12}	4.97× 10^{-12}	---	---	1.16× 10^{-11}	---	2.99× 10^{-11}	7.82× 10^{-11}	1.28× 10^{-10}
κ	0.112	0.110	0.119	---	---	0.117	---	0.120	0.149	0.171
k_{RPMD}	4.05× 10^{-14}	2.54× 10^{-13}	2.94× 10^{-13}	---	---	6.66× 10^{-13}	---	1.69× 10^{-12}	5.13× 10^{-12}	8.98× 10^{-12}

Figure 1. Minimum energy path (MEP) (Solid red lines) and the ground state adiabatic energy (blue dashed lines) for the reactions Cl + XCl (X=H, D, Mu) along the reaction coordinate.

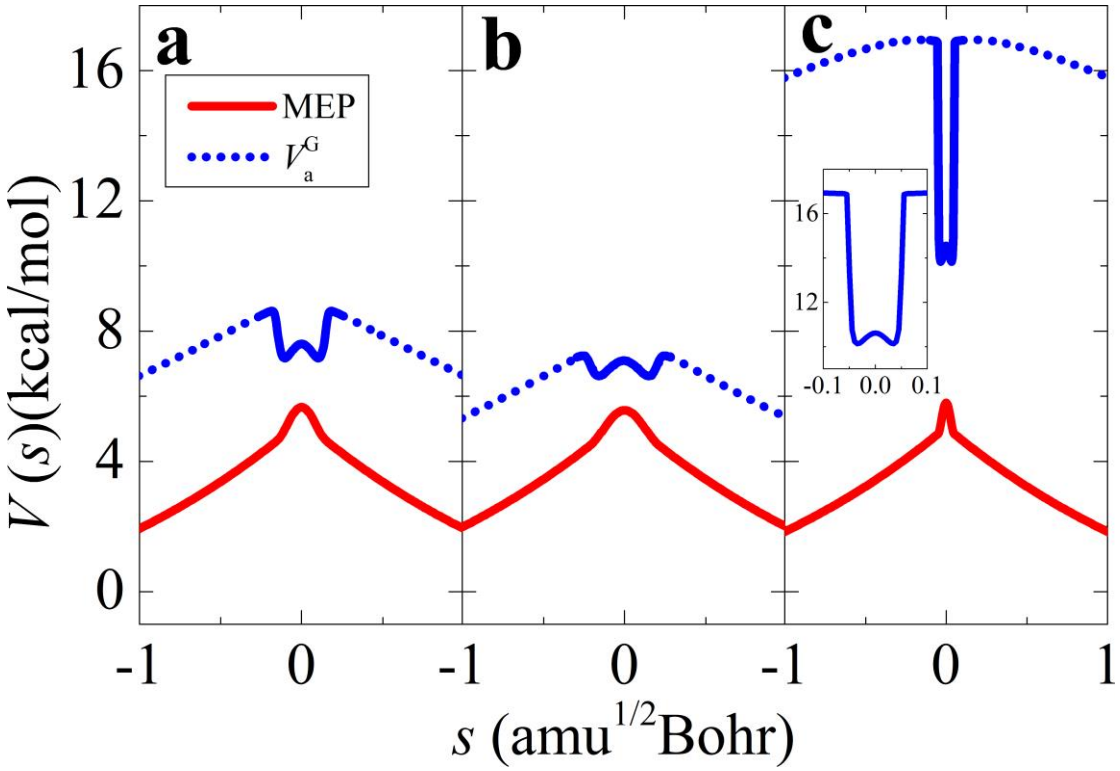

Figure 2. Potentials of mean force (PMF) (left panels) and transmission coefficients (right panels) of the Cl + XCl (X=H, D, Mu) reactions at 312.5 K.

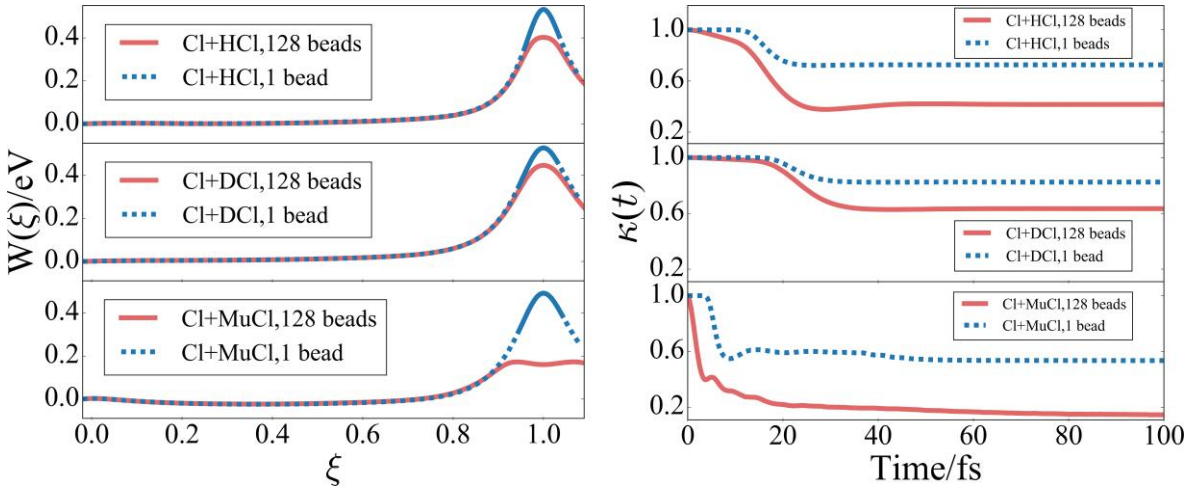

Figure 3. Comparison of rate coefficients gained by RPMD (Conv represents the converged number of beads, 1 bead represents that a single bead is used.), ICVT method, QD method, and experiments for the Cl + HCl reaction.

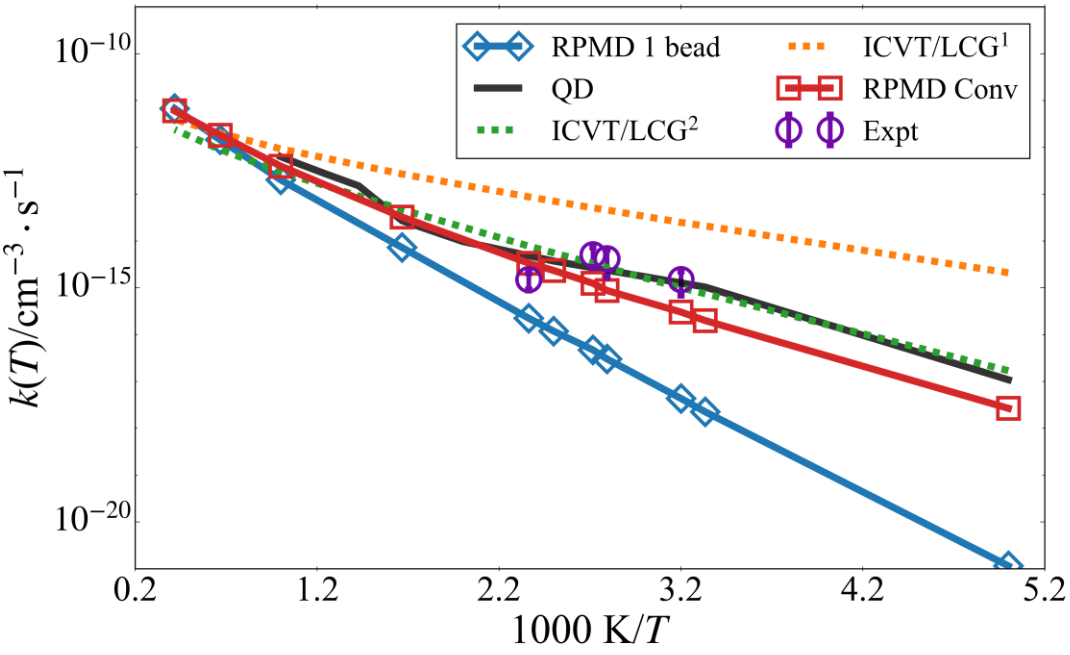

Figure 4. Comparison of rate coefficients gained by RPMD (Conv represents the converged number of beads, 1 bead represents that a single bead is used.), ICVT method and experiments for the Cl + DCl reaction.

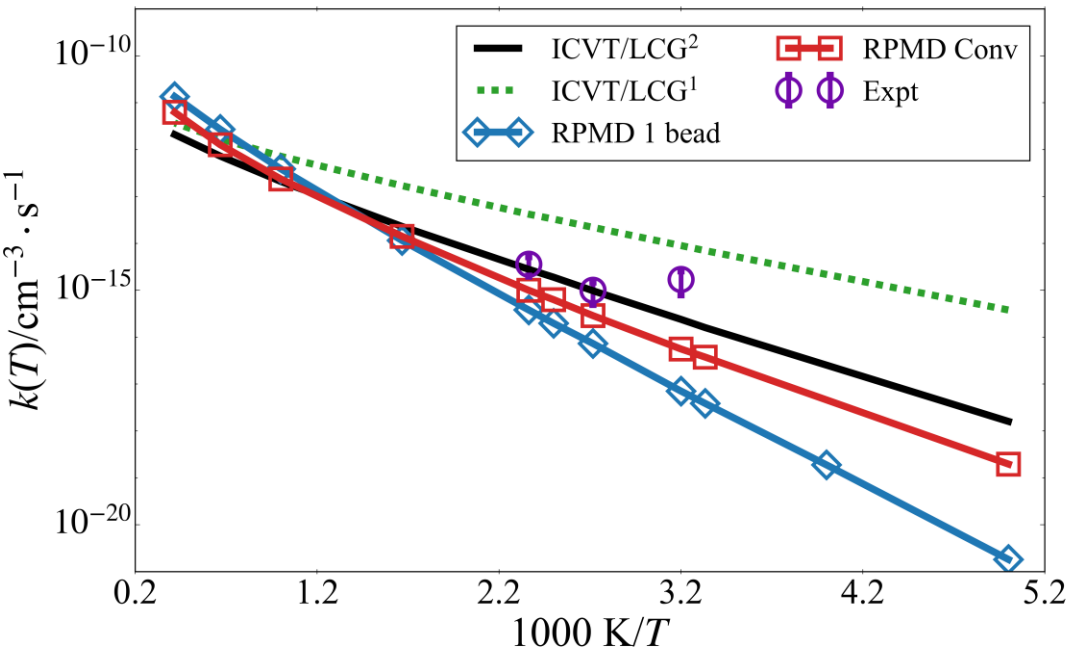

Figure 5. Comparison between calculated KIEs (k_H/k_D) and measured ones. Experimental data are taken from Bruce C. Garrett et al [44], and Other theoretical calculations results come from the reference[50].

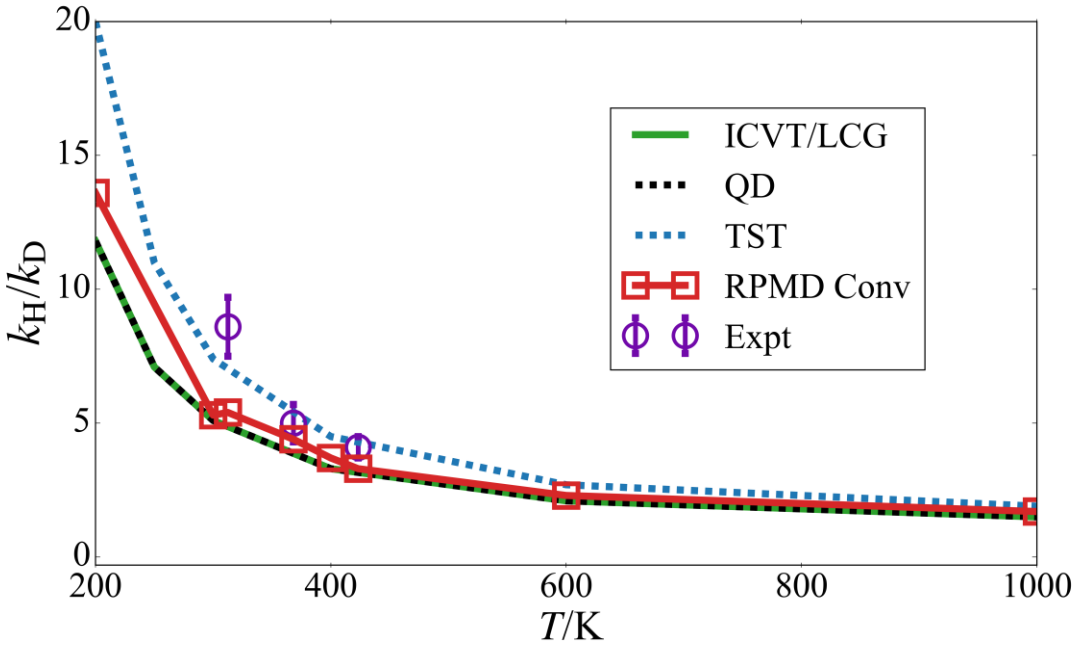

Reference

[1] D. G. G. Truhlar, Bruce C., Acc. Chem. Res. **13**, 440 (1980).

[2] S. C. Althorpe, and D. C. Clary, Annu. Rev. Phys. Chem. **54**, 493 (2003).

[3] H. Guo, Int. Rev. Phys. Chem. **31**, 1 (2012).

[4] J. Zuo, X. Hu, and D. Xie, Chinese. J. Chem. Phys. **31**, 123 (2018).

[5] A. Warshel, and Z. T. Chu, J. Chem. Phys. **93**, 4003 (1990).

[6] N. F. Hansen, and H. C. Andersen, J. Chem. Phys. **101**, 6032 (1994).

[7] E. Geva, Q. Shi, and G. A. Voth, J. Chem. Phys. **115**, 9209 (2001).

[8] W. H. Miller, Y. Zhao, M. Ceotto, and S. Yang, J. Chem. Phys. **119**, 1329 (2003).

[9] I. R. Craig, and D. E. Manolopoulos, J. Chem. Phys. **123**, 34102 (2005).

[10] S. J. Klippenstein, V. S. Pande, and D. G. Truhlar, J. Am. Chem. Soc. **136**, 528 (2014).

[11] Antonio Fernández-Ramos, J. A. Miller, and D. G. Truhlar, Chem. Rev. **106**, 4518 (2006).

[12] C. L. Vaillant, M. J. Thapa, J. Vaníček, and J. O. Richardson, J. Chem. Phys. **151**, 144111 (2019).

[13] J. M. Bowman, and G. C. Schatz, Annu. Rev. Phys. Chem. **46**, 169 (1995).

[14] Y. Li, Y. V. Suleimanov, and H. Guo, J. Phys. Chem. Lett. **5**, 700 (2014).

[15] R. P. de Tudela, Y. V. Suleimanov, M. Menendez, J. F. Castillo, and F. J. Aoiz, Phys. Chem. Chem. Phys. **16**, 2920 (2014).

[16] A. J. C. Varandas, Chem. Phys. Lett. **225**, 18 (1994).

[17] B. J. Braams, and D. E. Manolopoulos, J. Chem. Phys. **125**, 124105 (2006).

[18] I. R. Craig, and D. E. Manolopoulos, J. Chem. Phys. **121**, 3368 (2004).

[19] Y. V. Suleimanov, A. Aguado, S. Gomez-Carrasco, and O. Roncero, J. Phys. Chem. Lett. **9**, 2133 (2018).

[20] T. J. H. Hele, and S. C. Althorpe, J. Chem. Phys. **144**, 174107 (2016).

[21] S. L. Mielke, B. C. Garrett, D. G. Fleming, and D. G. Truhlar, Mol. Phys. **113**, 160 (2014).

[22] J. Aldegunde, P. G. Jambrina, E. García, V. J. Herrero, V. Sáez-Rábanos, and F. J. Aoiz, Mol. Phys. **111**, 3169 (2013).

[23] Y. V. Suleimanov, J. W. Allen, and W. H. Green, Comput. Phys. Commun. **184**, 833 (2013).

[24] Y. V. Suleimanov, R. Collepardo-Guevara, and D. E. Manolopoulos, J. Chem. Phys. **134**, 044131 (2011).

[25] D. Chandler, J. Chem. Phys. **68**, 2959 (1978).

[26] W. H. Miller, S. D. Schwartz, and J. W. Tromp, J. Chem. Phys. **79**, 4889 (1983).

[27] R. Collepardo-Guevara, Y. V. Suleimanov, and D. E. Manolopoulos, J. Chem. Phys. **130**, 219901 (2009).

[28] J. Kastner, and W. Thiel, J. Chem. Phys. **123**, 144104 (2005).

[29] R. Collepardo-Guevara, Y. V. Suleimanov, and D. E. Manolopoulos, J. Chem. Phys. **130**, 174713 (2009).

[30] T. E. Markland, and D. E. Manolopoulos, J. Chem. Phys. **129**, 024105 (2008).

[31] J. O. Richardson, and S. C. Althorpe, J. Chem. Phys. **131**, 214106 (2009).

[32] R. Perez de Tudela, F. J. Aoiz, Y. V. Suleimanov, and D. E. Manolopoulos, J. Phys. Chem. Lett. **3**, 493 (2012).

[33] Y. Li, Y. V. Suleimanov, J. Li, W. H. Green, and H. Guo, J. Chem. Phys. **138**, 094307 (2013).

[34] D. K. Bondi, J. N. L. Connor, J. Manz, and J. Römelt, Mol. Phys. **50**, 467 (1983).

[35] R. J, *Calculations on Collinear Reactions Using Hyperspherical Coordinates*, New York: Springer-Dordrecht,77 (1986).

[36] H. C. Andersen, J. Comput. Phys. **52**, 24 (1983).

[37] J. P. Ryckaert, G. Ciccotti, and H. J. C. Berendsen, J. Comput. Phys. **23**, 327 (1977).

[38] B. C. Garrett, and D. G. Truhlar, J. Phys. Chem. **83**, 1052 (1979).

[39] T. G. Yang, J. Chen, L. Huang, T. Wang, C. L. Xiao, Z. G. Sun, D. X. Dai, X. M. Yang, and D. H. Zhang, Science. **347**, 60 (2015).

[40] E. Merzbacher, *Quantum Mechanics*, New York: John Wiley & Sons,(1998).

[41] D.-N. Le, N.-T. D. Hoang, and V.-H. Le, J. math. phys. **59**, 032101 (2018).

[42] Y. V. Suleimanov, R. P. de Tudela, P. G. Jambrina, J. F. Castillo, V. Saez-Rabanos, D. E. Manolopoulos, and F. J. Aoiz, Phys. Chem. Chem. Phys. **15**, 3655 (2013).

[43] D. G. Fleming, D. J. Arseneau, O. Sukhorukov, J. H. Brewer, S. L. Mielke, G. C. Schatz, B. C. Garrett, K. A. Peterson, and D. G. Truhlar, Science. **331**, 448 (2011).

[44] B. C. Garrett, D. G. Truhlar, A. F. Wagner, and T. H. Dunning, J. Chem. Phys. **78**, 4400 (1983).

[45] R. Collepardo-Guevara, Y. V. Suleimanov, and D. E. Manolopoulos, J Chem Phys **130**, 174713 (2009).

[46] Y. V. Suleimanov, F. J. Aoiz, and H. Guo, J. Phys. Chem. A. **120**, 8488 (2016).

[47] X. M. Yang, and D. H. Zhang, Accounts. Chem. Res. **41**, 981 (2008).

[48] W. R. Dong, C. L. Xiao, T. Wang, D. X. Dai, X. M. Yang, and D. H. Zhang, Science **327**, 1501 (2010).

[49] T. Yang, L. Huang, C. Xiao, J. Chen, T. Wang, D. Dai, F. Lique, M. H. Alexander, Z. Sun, D. H. Zhang, X. Yang, and D. M. Neumark, Nat. Chem. **11**, 744 (2019).

[50] D. K. Bondi, J. N. L. Connor, B. C. Garrett, and D. G. Truhlar, J. Chem. Phys. **78**, 5981 (1983).